measurements strongly rule out a source dominated by material synthesized by the s-process ("sp-" models in Fig. 2), on the basis of Hg and Pb abundances and the presence of actinides, which are not produced by the s-process at all (Fig. 2). Using HEAO data, Binns *et al.*[8] did not rule out an s-process source based on Sn, Te and Ba abundances. In an analysis of measurements of GCR composition using the HEAO-3[23] and Ariel-6[19] instruments, Binns *et al.*[8] have proposed an empirical model in which GCRs with $Z < 60$ have a solar-like composition, but those with $Z > 60$ are dramatically enhanced in r-process material. Our data are consistent with a source consisting of freshly synthesized r-process material with FIP-ordered preferential acceleration ("rp-fip" in Fig. 2). Although an r-process enhancement might be expected in supernova ejecta, no detailed model has been proposed which gives such an enhancement only for $Z > 60$. However, there is some indication from presolar abundances of ^{129}I and ^{182}Hf of an r-process component which preferentially synthesizes nuclei with atomic weight $A > 140$ ($Z \geqslant 58$)[24].

Ramaty, Lingenfelter and Kozolvsky have recently suggested that GCRs originate in grains condensed from fresh supernova ejecta[25]. Such a source would be enriched in r-process material and refractory elements (qualitatively similar to "rp-vol" in Fig. 2). A pure r-process source with $\geqslant 1.5$ acceleration bias is inconsistent with the observed Pb abundance.

The interstellar grain plus gas model of Meyer, Drury and Ellison[6,7], and the empirical r-process enhancement model of Binns *et al.*[8] discussed above predict very similar Hg and Pb abundances (Fig. 2), but they could be distinguished by a more accurate measurement of the overall actinide abundances. Also, freshly synthesized r-process material, predicted by the Binns *et al.* model and by Ramaty, Lingenfelter and Kozlovsky[25], would necessarily be young, and the unstable actinides (Th, U, Pu, Cm) could serve as 'clocks' to measure the age of the nuclei. The actinides are quite rare, so an exposure of $\sim$100 m^2 yr sr is required to accurately measure age. ECCO, a detector similar to Trek currently under study for deployment on the International Space Station, is expected to have sufficient collecting power and charge resolution to achieve this goal. □

Received 15 June; accepted 28 July 1998.

1. Zweibel, E. G. & Heiles, C. Magnetic fields in galaxies and beyond. *Nature* **385,** 131–136 (1997).
2. McKee, C. F., Zweibel, E. G., Heiles, C. & Goodman, A. A. in *Protostars and Planets III* (eds Levy, E. H. & Lunine, J. I.) 327–366 (Univ. Arizona Press, Tucson, 1993).
3. Gaisser, T. K. *Cosmic Rays and Particle Physics* (Cambridge Univ. Press, 1990).
4. Webber, W. R. New experimental data and what it tells us about the sources and acceleration of cosmic rays. *Space Sci. Rev.* **81,** 107–142 (1997).
5. Meyer, J.-P. Solar-stellar outer atmospheres and energetic particles, and galactic cosmic rays. *Astrophys. J. Suppl.* **57,** 173–204 (1985).
6. Meyer, J.-P., Drury, L. O'C. & Ellison, D. C. Galactic cosmic rays from supernova remnants. I. A cosmic-ray composition controlled by volatility and mass-to-charge ratio. *Astrophys. J.* **487,** 182–196 (1997).
7. Ellison, D. C., Meyer, J.-P. & Drury, L. O'C. Galactic cosmic rays from supernova remnants. II. Shock acceleration of gas and dust. *Astrophys. J.* **487,** 197–217 (1997).
8. Binns, W. R. *et al.* in *Cosmic Abundances of Matter* (ed. Waddington, C. J.) 147–167 (Am. Inst. Physics, New York, 1989).
9. Meyer, B. S. The r-, s-, and p-processes. *Annu. Rev. Astron. Astrophys.* **32,** 153–190 (1994).
10. Wang, S.-C. *et al.* Phosphate glass detectors with high sensitivity to nuclear particles. *Nucl. Instrum. Meth. B* **35,** 43–49 (1988).
11. Fleischer, R. L., Price, P. B. & Walker, R. M. *Nuclear Tracks in Solids* (Univ. California Press, Berkeley, 1975).
12. Westphal, A. J. & He, Y. D. Measurement of cross sections for electron capture and stripping by highly relativistic ions. *Phys. Rev. Lett.* **71,** 1160–1163 (1993).
13. Westphal, A. J., Price, P. B. & Snowden-Ifft, D. P. Upper limit on the cross section for nuclear charge pickup by relativistic uranium ions. *Phys. Rev. C* **45,** 2423–2426 (1992).
14. Weaver, B. A. *et al.* Performance of the ultraheavy collector of the Trek experiment. *Nucl. Instrum. Meth.* (submitted).
15. Möller, P. & Nix, J. R. Stability and decay of nuclei at the end of the periodic system. *J. Phys. G* **20,** 1681–1747 (1994).
16. Geer, L. Y. *et al.* Charge-changing fragmentation of 10.6 GeV/nucleon ^{197}Au nuclei. *Phys. Rev. C* **52,** 334–345 (1995).
17. Clinton, R. R. & Waddington, C. J. Dependence of the interstellar propagation of ultraheavy cosmic-ray nuclei on various parameters *Astrophys. J.* **403,** 644–657 (1993).
18. Reames, D. V. Coronal abundances determined from energetic particles. *Adv. Space Res.* **15,** 41–51 (1995).
19. Fowler, P. H. *et al.* Ariel 6 measurements of the fluxes of ultraheavy cosmic rays. *Astrophys. J.* **314,** 739–746 (1987).
20. O'Sullivan, D., Thompson, A., Keane, A. J., Drury, L. O'C. & Wenzel, K.-P. Investigation of $Z \geq 70$ cosmic ray nuclei on the LDEF mission. *Radiat. Meas.* **26,** 889–892 (1996).
21. Epstein, R. I. The acceleration of interstellar grains and the composition of the cosmic rays. *Mon. Not. R. Astron. Soc.* **193,** 723–729 (1980).
22. Cesarsky, C. J. & Bibring, J. P. in *Origin of Cosmic Rays* (eds Setti, G., Spada, G. & Wolfendale, A. W.) 361–362 (IAU Symp. 94, Reidel, Dordrecht, 1980).
23. Binns, W. R. *et al.* Abundances of ultraheavy elements in the cosmic radiation: results from HEAO 3. *Astrophys. J.* **346,** 997–1009 (1989).
24. Wasserburg, G. J., Busso, M. & Gallino, R. Abundances of actinides and short-lived nonactinides in the interstellar medium: diverse supernova sources for the r-processes. *Astrophys. J.* **466,** L109–113 (1996).
25. Ramaty, R., Kozlovsky, B. & Lingenfelter, R. Cosmic rays, nuclear gamma rays and the origin of the light elements. *Phys. Today* **51,** 30–35 (1998).
26. Takahashi, K., Boyd, R. N., Mathews, G. J. & Yokoi, K. Bound-state beta decay of highly ionized atoms. *Phys. Rev. C* **36,** 1522–1528 (1987).
27. Anders, E. & Grevesse, N. Abundances of the elements: meteoritic and solar. *Geochim. Cosmochim. Acta* **53,** 197–214 (1989).
28. Pfeiffer, K., Kratz, K.-L. & Thielemann, F.-K. Analysis of the solar-system r-process abundance pattern with the new ETFSI-Q mass formula. *Z. Phys. A* **357,** 235–238 (1997).
29. Käppeler, F., Beer, H. & Wisshak, K. s-process nucleosynthesis—nuclear physics and the classical model. *Rep. Prog. Phys.* **52,** 945–1013 (1989).
30. Beer, H., Corvi, F. & Mutti, P. Neutron capture of the bottleneck isotopes ^{138}Ba and ^{208}Pb, s-process studies, and the r-process abundance distribution. *Astrophys. J.* **474,** 843–861 (1997).

Acknowledgements. We thank D. O'Sullivan, M. Solarz, V. Akimov, Y. He, the staff at the AGS, and the crews of Mir and STS-74 for their assistance. We also thank the UHIC collaboration for providing measured cross-sections, and C. J. Waddington, B. S. Mayer and J.-P. Meyer for calculations and discussions.

Correspondence and requests for materials should be addressed to A.W. (e-mail: westphal@dilbert.berkeley.edu).

Complete quantum teleportation using nuclear magnetic resonance

M. A. Nielsen*†, E. Knill‡ & R. Laflamme*

** Theoretical Astrophysics T-6, MS B-288, and ‡ Computer Research and Applications CIC-3, MS B-265, Los Alamos National Laboratory, Los Alamos, New Mexico 87545, USA*

† Department of Physics and Astronomy, University of New Mexico, Albuquerque, New Mexico 87131-1131, USA

Quantum-mechanical systems have information processing capabilities[1,2] that are not possible with classical devices. One example is quantum teleportation[3], in which the quantum state of a system is transported from one location to another without moving through the intervening space. But although partial implementations[4,5] of quantum teleportation over macroscopic distances have been achieved using optical systems, the final stage of the teleportation procedure—which allows the complete recovery of the original state—was omitted. Here we report an experimental implementation of full quantum teleportation over interatomic distances using liquid-state nuclear magnetic resonance. We achieve teleportation of the quantum state of a carbon nucleus to a hydrogen nucleus in molecules of trichloroethylene, by exploiting natural phase decoherence of the carbon nuclei. Such a teleportation scheme may be used as a subroutine in larger quantum computations, or for quantum communication.

In classical physics, an object can be teleported, in principle, by performing a measurement to characterize completely the properties of the object. That information can then be sent to another location, and the object reconstructed. Does this provide a complete reconstruction of the original object? No: all physical systems are ultimately quantum mechanical, and quantum mechanics tells us that it is impossible to determine completely the state of an unknown quantum system, making it impossible to use the classical measurement procedure to move a quantum system from one location to another.

Bennett *et al.*[3] have suggested a procedure for teleporting quantum states. Quantum teleportation may be described abstractly in terms of two parties, Alice and Bob. Alice has in her possession an unknown state $|\Psi\rangle = \alpha|0\rangle + \beta|1\rangle$ of a single quantum bit (qubit)—a two-level quantum system. The goal of teleportation is to trans-

port the state of that qubit to Bob. In addition, Alice and Bob each possess one qubit of a two-qubit entangled state;

$$|\Psi\rangle_A(|0\rangle_A|0\rangle_B + |1\rangle_A|1\rangle_B) \quad (1)$$

where subscripts A are used to denote Alice's systems, and subscripts B to denote Bob's systems. Here and throughout we omit overall normalization factors from our equations.

This state can be rewritten in the Bell basis ($(|00\rangle \pm |11\rangle)$, $(|01\rangle \pm |10\rangle)$) for the first two qubits and a conditional unitary transformation of the state $|\Psi\rangle$ for the last one, that is;

$$\begin{aligned}&(|00\rangle + |11\rangle)|\Psi\rangle + (|00\rangle - |11\rangle)\sigma_z|\Psi\rangle \\ &+ (|01\rangle + |10\rangle)\sigma_x|\Psi\rangle + (|01\rangle - |10\rangle)(-i\sigma_y|\Psi\rangle)\end{aligned} \quad (2)$$

where σ_x, σ_y, σ_z are the Pauli sigma operators[6], in the $|0\rangle$, $|1\rangle$ basis. A measurement is performed on Alice's qubits in the Bell basis. Conditional on these measurement outcomes it may be verified from equation (2) that Bob's respective states are:

$$|\Psi\rangle; \quad \sigma_z|\Psi\rangle; \quad \sigma_x|\Psi\rangle; \quad -i\sigma_y|\Psi\rangle \quad (3)$$

Alice sends the outcome of her measurement to Bob, who can then recover the original state $|\Psi\rangle$ by applying the appropriate unitary transformation I, σ_z, σ_x or $i\sigma_y$, conditional on Alice's measurement outcome. We note that the quantum state transmission has not been accomplished faster than light because Bob must wait for Alice's measurement result to arrive before he can recover the quantum state.

Recent demonstrations of quantum teleportation[4,5] omitted the final stage of teleportation, the unitary operators applied by Bob conditional on the result of Alice's measurement. This prevents complete recovery of the original state. Instead, the earlier experiments relied on classical post-processing of the data after completion of the experiment to check that the results were consistent with what one would expect if the conditional operations had, in fact, been performed. Our experiment implements the full teleportation operation. The most important implication of the inclusion of this extra stage is that our teleportation procedure can, in principle, be used as a subroutine in the performance of other quantum information processing tasks. Teleportation as a subroutine is important in potential applications to quantum computation and communication[7,8], although in our experimental system, moving Alice's qubit to Bob may be accomplished more efficiently by techniques other than teleportation.

Our implementation of teleportation is performed using liquid-state nuclear magnetic resonance (NMR), applied to an ensemble of molecules of labelled trichloroethylene (TCE). The structure of the TCE molecule may be depicted as:

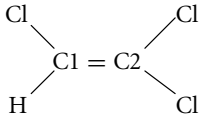

(4)

To perform teleportation we make use of the hydrogen nucleus (H), and the two ^{13}C nuclei (C1 and C2), teleporting the state of C2 to H. Figure 1a illustrates the teleportation process we used. The circuit has three inputs, which we will refer to as the data (C2), ancilla (C1) and target (H) qubits. The goal of the circuit is to teleport the state of the data qubit so that it ends up on the target qubit. We are therefore only teleporting the qubit a few ångstroms, making this a demonstration of the method of teleportation, rather than a practical means for transmitting qubits over long distances.

State preparation is done in our experiment using the gradient-pulse techniques described by Cory *et al.*[9], and phase cycling[10,11]. The unitary operations performed during teleportation may be implemented in a straightforward manner in NMR, using non-selective radio frequency (r.f.) pulses tuned to the Larmor frequencies of the nuclear spins, and delays allowing entanglement to form through the interaction of neighbouring nuclei[9,12]. Other demonstrations of quantum information processing with three qubits using NMR are described in refs 13–15, and with two qubits in refs 16–19.

An innovation in our experiment was the method used to implement the Bell basis measurement. In NMR, the measurement step allows us to measure the expectation values of σ_x and σ_y for each spin, averaged over the ensemble of molecules, rather than performing a projective measurement in some basis. For this reason, we must modify the projective measurement step in the standard description of teleportation, while preserving the teleportation effect.

We use a procedure inspired by Brassard *et al.*[20], who suggest a two-part procedure for performing the Bell basis measurement. Part one of the procedure is to rotate from the Bell basis into the computational basis, $|00\rangle$, $|01\rangle$, $|10\rangle$, $|11\rangle$. We implement this step in NMR by using the natural spin–spin coupling between the carbon nuclei, and r.f. pulses. Part two of the procedure is to perform a projective measurement in the computational basis. As Brassard *et al.* point out, the effect of this two-part procedure is equivalent to performing the Bell basis measurement, and leaving the data and ancilla qubits in one of the four states, $|00\rangle$, $|01\rangle$, $|10\rangle$, $|11\rangle$, corresponding to the different measurement results.

We cannot directly implement the second step in NMR. Instead, we exploit the natural phase decoherence occurring on the carbon nuclei to achieve the same effect. We note that phase decoherence completely randomizes the phase information in these nuclei and thus will destroy coherence between the elements of the above basis. Its effect on the state of the carbon nuclei is to diagonalize the state in the computational basis. In terms of the density matrix ρ for the carbon nuclei this process may be expressed as:

$$\begin{aligned}\rho \longrightarrow &|00\rangle\langle 00|\rho|00\rangle\langle 00| + |01\rangle\langle 01|\rho|01\rangle\langle 01| + |10\rangle\langle 10|\rho|10\rangle\langle 10| \\ &+ |11\rangle\langle 11|\rho|11\rangle\langle 11|\end{aligned} \quad (5)$$

As emphasized by Zurek[21], the decoherence process is indistinguishable from a measurement in the computational basis for the carbons accomplished by the environment. We do not observe the result of this measurement explicitly, but the state of nuclei selected by the decoherence process contains the measurement result, and therefore we can do the final transformation conditional on the particular state the environment has selected. As in the scheme of Brassard *et al.*, the final state of the carbon nuclei is one of the four states, $|00\rangle$, $|01\rangle$, $|10\rangle$, $|11\rangle$, corresponding to the four possible results of the measurement.

Our experiment exploits the natural decoherence properties of the TCE molecule. The phase decoherence times (T_2) for C1 and C2 are approximately 0.4 s and 0.3 s. All other T_2 and T_1 times for all three nuclei are much longer, with a T_2 time for the hydrogen of ~3 s, and relaxation times (T_1) of approximately 20–30 s for the carbons, and 5 s for the hydrogen.

Thus, for delays of the order of 1 s, we can approximate the total evolution by exact phase decoherence on the carbon nuclei. The total scheme therefore implements a measurement in the Bell basis, with the result of the measurement stored as classical data on the carbon nuclei following the measurement. We can thus teleport the state from the carbon to the hydrogen and verify that the final state decays at the hydrogen rate and not the carbon rate.

Re-examining Fig. 1a we see how remarkable teleportation is from this point of view. During the stage labelled "measure in the Bell basis" in Fig. 1a, we allow the C1 and C2 nuclei to decohere and thus be measured by the environment, destroying all phase information on the data and ancilla qubits. Experimentally, a standard NMR technique known as refocusing employs r.f. pulses to ensure that the data qubit effectively does not interact with the target qubit. Classical intuition therefore tells us that the phase information about the input state, $|\Psi\rangle$, has been lost forever. Nevertheless, quantum mechanics predicts that we are still able

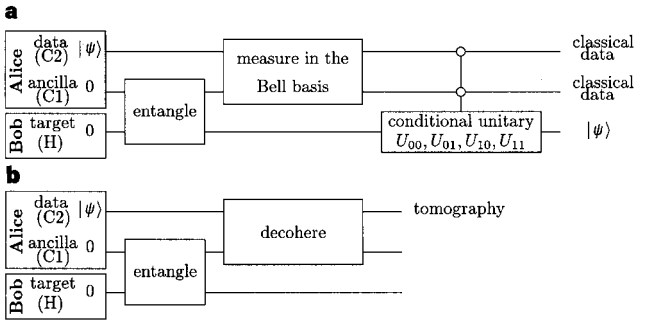

Figure 1 Schematic circuits for the quantum teleportation experiment (**a**) and the control experiment (**b**). The teleportation circuit is based on that suggested by Brassard *et al.*[20] We note that the control circuit omits two elements of the teleportation experiment–rotation from the Bell basis into the computational basis, immediately before the decoherence step, and the conditional unitary operation. Pulse sequences for our experiment are available at http://wwwcas.phys.unm.edu/~mnielsen/nmr/index.html

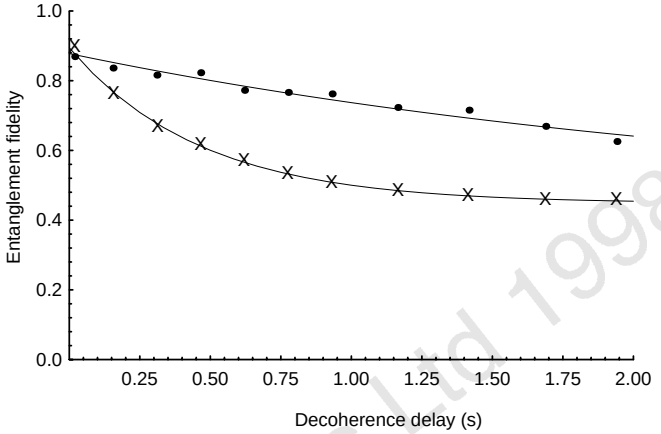

Figure 2 Entanglement fidelity (a measure of how well quantum information is preserved) plotted as a function of decoherence delay. The bottom curve is a control run where the information remains in C2; the curve shows a decay time of ~0.5 s. The top curve represents the fidelity of the quantum teleportation process. The decay time is ~2.6 s. The information is preserved for a longer time, corresponding approximately to the combined effects of decoherence and relaxation for the hydrogen, confirming the prediction of teleportation.

to recover the complete system after this decoherence step, by quantum teleportation.

We implemented this scheme in TCE using a Bruker DRX-500 NMR spectrometer. Experimentally, we determined the Larmor and coupling frequencies for the hydrogen, C1 and C2 to be:

$$\omega_H \approx 500.133491\ \text{MHz}; \quad \omega_{C1} \approx 125.772580\ \text{MHz}; \quad \omega_{C2} \approx \omega_{C1} - 911\ \text{Hz} \tag{6}$$

$$J_{HC1} \approx 201\ \text{Hz}; \quad J_{C1C2} \approx 103\ \text{Hz} \tag{7}$$

The coupling frequencies between H and C2, as well as the chlorines to H, C1 and C2, are much lower, of the order of 10 Hz for the former, and less than 1 Hz for the latter. Experimentally, these couplings are suppressed by multiple refocusings, and will be ignored in the sequel. We note that C1 and C2 have slightly different frequencies, due to the different chemical environments of the two atoms.

We performed two separate sets of experiments. In one set, the full teleportation process was executed, making use of a variety of decoherence delays in place of the measurement. The readout was performed on the hydrogen nucleus, and a figure of merit—the entanglement fidelity—was calculated for the teleportation process. The entanglement fidelity is a quantity in the range 0–1 which measures the combined strength of all noise processes occurring during the process[22,23]. (In the notation of ref. 22, we calculate $F_e(I/2,\varepsilon)$, where ε is the teleportation operation.) In particular, an entanglement fidelity of 1 indicates perfect teleportation, while an entanglement fidelity of 0.25 indicates total randomization of the state. Perfect 'classical transmission' corresponds to an entanglement fidelity of 0.5 (refs 22, 23), so entanglement fidelities greater than 0.5 indicate that teleportation of some quantum information is taking place.

The second set of experiments was a control set (Fig. 1b). In these experiments, only the state preparation and initial entanglement of H and C1 were performed, followed by a delay for decoherence on C1 and C2. The readout was performed in this instance on C2, and the entanglement fidelity was calculated for the process.

The results of our experiment are shown in Fig. 2, where the entanglement fidelity is plotted against the decoherence delay. Errors in our experiment arise from the strong coupling effect, imperfect calibration of r.f. pulses, and r.f. field inhomogeneities. The estimated uncertainties in the entanglement fidelities are less than ± 0.05, and are due primarily to r.f. field inhomogeneity and imperfect calibration of r.f. pulses.

To determine the entanglement fidelities for the teleportation and control experiments, we performed 'quantum process tomography' (refs 24, 25), a procedure for obtaining a complete description of the dynamics of a quantum system, as follows: the linearity of quantum mechanics implies that the single-qubit input and output for the teleportation process are related by a linear quantum operation[26]. By preparing a complete set of four linearly independent initial states, and measuring the corresponding states output from the experiment, we may completely characterize the quantum process, enabling us to calculate the entanglement fidelity for the process[25].

We note three elements in Fig. 2. First, for small decoherence delays, the entanglement fidelity for the teleportation experiments significantly exceeds the value of 0.5 for perfect classical transmission of data, indicating successful teleportation of quantum information from C2 to H, with reasonable fidelity. Second, the entanglement fidelity decays very quickly for the control experiments as the delay is increased. Theoretically, we expect this to be the case, due to a T_2 time for C2 of ~0.3 s. Third, the decay of the entanglement fidelity for the teleportation experiments occurs much more slowly. Theoretically, we expect this decay to be due mainly to the effect of phase decoherence and relaxation on the hydrogen. Our experimental observations are consistent with this prediction, and provide more support for the claim that quantum data are being teleported in these experiments.

Note added in proof: Since completing this work we have become aware of related work by Furusawa *et al.*[27]. □

Received 7 July; accepted 15 October 1998.

1. Bennett, C. H. Quantum information and computation. *Phys. Today* **48,** 24–30 (1995).
2. Preskill, J. Quantum computing: pro and con. *Proc. R. Soc. Lond. A* **454,** 469–486 (1998).
3. Bennett, C. H. *et al.* Teleporting an unknown quantum state via dual classical and EPR channels. *Phys. Rev. Lett.* **70,** 1895–1899 (1993).
4. Bouwmeester, D. *et al.* Experimental quantum teleportation. *Nature* **390,** 575–579 (1997).
5. Boschi, D., Branca, S., De Martini, F., Hardy, L. & Popescu, S. Experimental realization of teleporting an unknown pure quantum state via dual classical and Einstein-Podolski-Rosen channels. *Phys. Rev. Lett.* **80,** 1121–1125 (1998).
6. Sakurai, J. J. *Modern Quantum Mechanics* (Addison-Wesley, Reading, MA, 1995).
7. Bennett, C. H., DiVencenzo, D. P., Smolin, J. A. & Wootters, W. K. Mixed state entanglement and quantum error correction. *Phys. Rev. A* **54,** 3824–3851 (1996).
8. Cirac, J. I., Zoller, P., Kimble, H. J. & Mabuchi, H. Quantum state transfer and entanglement distribution among distant nodes in a quantum network. *Phys. Rev. Lett.* **78,** 3221–3224 (1997).
9. Cory, D. G., Fahmy, A. F. & Havel, T. F. Ensemble quantum computing by NMR spectroscopy. *Proc. Natl Acad. Sci. USA* **94,** 1634–1639 (1997).

10. Ernst, R., Bodenhausen, G. & Wokaun, A. *Principles of Nuclear Magnetic Resonance in One and Two Dimensions* (Oxford Univ. Press, 1990).
11. Grant, D. M. & Harris, R. K. (eds) *Encyclopedia of Nuclear Magnetic Resonance* (Wiley, New York, 1996).
12. Gershenfeld, N. & Chuang, I. L. Bulk spin resonance quantum computation. *Science* **275,** 350–356 (1997).
13. Cory, D. G., Price, M. D. & Havel, T. F. Nuclear magnetic resonance spectroscopy: An experimentally accessible paradigm for quantum computing. *Physica D* **120,** 82–101 (1998).
14. Laflamme, R., Knill, E., Zurek, W. H., Catasti, P. & Mariappan, S. V. S. NMR Greenberger-Horne-Zeilinger states. *Phil. Trans. R. Soc. Lond. A* **356,** 1941–1947 (1998).
15. Cory, D. G. *et al*. Experimental quantum error correction. *Phys. Rev. Lett.* **81,** 2152–2155 (1998).
16. Chuang, I. L., Gershenfeld, N. & Kubinec, M. Experimental implementation of fast quantum searching. *Phys. Rev. Lett.* **18,** 3408–3411 (1998).
17. Jones, J. A. & Mosca, M. Implementation of a quantum algorithm on a nuclear magnetic resonance quantum computer. *J. Chem. Phys.* **109,** 1648–1653 (1998).
18. Chuang, I. L., Vandersypen, L. M. K., Zhou, X. L., Leung, D. W. & Lloyd, S. Experimental realization of a quantum algorithm. *Nature* **393,** 143–146 (1998).
19. Jones, J. A., Mosca, M. & Hansen, R. H. Implementation of a quantum search algorithm on a nuclear magnetic resonance quantum computer. *Nature* **393,** 344–346 (1998).
20. Brassard, G., Braunstein, S. & Cleve, R. Teleportation as a quantum computation. *Physica D* **120,** 43–47 (1998).
21. Zurek, W. H. Decoherence and the transition from quantum to classical. *Phys. Today* **44,** 36–44 (1991).
22. Schumacher, B. W. Sending entanglement through noisy quantum channels. *Phys. Rev. A* **54,** 2614–2628 (1996).
23. Barnum, H., Nielsen, M. A. & Schumacher, B. W. Information transmission through a noisy quantum channel. *Phys. Res. A* **57,** 4153–4175 (1998).
24. Poyatos, J. F., Cirac, J. I. & Zoller, P. Complete characterization of a quantum process: the two-bit quantum gate. *Phys. Rev. Lett.* **78,** 390–393 (1997).
25. Chuang, I. L. & Nielsen, M. A. Prescription for experimental determination of the dynamics of a quantum black box. *J. Mod. Opt.* **44,** 2455–2467 (1997).
26. Nielsen, M. A. & Caves, C. M. Reversible quantum operations and their application to teleportation. *Phys. Rev. A* **55,** 2547–2556 (1997).
27. Furusawa, A. *et al*. Unconditional quantum teleportation. *Science* (in the press).

Acknowledgements. We thank D. Cory, C. Jarzynski, J. Ye and W. Zurek for discussions, the Stable Isotope Laboratory at Los Alamos for use of their facility, and the National Security Agency and Office of Naval Research for support.

Correspondence and requests for materials should be addressed to M.A.N. (e-mail: mnielsen@theory.caltech.edu).

Experimental verification of the quasi-unit-cell model of quasicrystal structure

Paul J. Steinhardt*, H.-C. Jeong†, K. Saitoh‡, M. Tanaka‡, E. Abe§ & A. P. Tsai§

* *Department of Physics, Princeton University, Princeton, New Jersey 08544, USA*
† *Department of Physics, Sejong University, Kwangjin, Seoul 143-747, Korea*
‡ *Research Institute for Scientific Measurements, Tohoku University, 2-1-1 Katahira, Aoba-ku, Sendai 980-8577, Japan*
§ *National Research Institute for Metals, 1-2-1 Sengen, Tsukuba, Ibaraki 305-0047, Japan*

The atomic structure of quasicrystals[1]—solids with long-range order, but non-periodic atomic lattice structure—is often described as the three-dimensional generalization of the planar two-tile Penrose pattern[2]. Recently, an alternative model has been proposed[3–5] that describes such structures in terms of a single repeating unit[3–5]—the three-dimensional generalization of a pattern composed of identical decagons. This model is similar in concept to the unit-cell description of periodic crystals, with the decagon playing the role of a 'quasi-unit cell'. But, unlike the unit cells in periodic crystals, these quasi-unit cells overlap their neighbours, in the sense that they share atoms. Nevertheless, the basic concept of unit cells in both periodic crystals and quasicrystals is essentially the same: solving the entire atomic structure of the solid reduces to determining the distribution of atoms in the unit cell. Here we report experimental evidence for the quasi-unit-cell model by solving the structure of the decagonal quasicrystal $Al_{72}Ni_{20}Co_8$. The resulting structure is consistent with images obtained by electron and X-ray diffraction, and agrees with the measured stoichiometry, density and symmetry of the compound. The quasi-unit-cell model provides a significantly better fit to these results than all previous alternative models, including Penrose tiling.

The fact that the entire structure reduces to a single repeating unit means that quasicrystals have a simplicity more like that of crystals than previously recognized. The quasi-unit-cell picture also suggests reasons why quasicrystals may form instead of crystals under some conditions. For the two-dimensional analogue, a pattern composed of overlapping decagonal quasi-unit cells, Gummelt[3] and Steinhardt and Jeong[4,5] have proved that the quasicrystal pattern is uniquely forced if decagons only overlay according to the rules shown in Fig. 1a. Steinhardt and Jeong[4,5] have further proved that the quasi-unit-cell structure can arise simply by maximizing the density of a chosen cluster of atoms. If one imagines that the atomic cluster is energetically preferred, then the quasicrystal could be the ground-state configuration as minimizing the free energy maximizes the cluster density. Establishing the correspondence between quasi-unit cells and real atomic structures opens the door to theoretical and empirical tests of these notions.

The quasi-unit-cell and Penrose-tile pictures are examples of real-space descriptions of quasicrystals in which the structure is defined by decorating each quasi-unit cell or each type of tile identically. Some Penrose-tile models are based on the two-tile rhombus or kite-and-dart sets; others are based on the six-tile pentagonal set. In the hyperspace description, the quasicrystal is viewed as a projection from a higher-dimensional periodic, hypercubic lattice and the atomic decoration is defined in terms of atomic surfaces in the higher-dimensional space (five or six dimensions) which project into point atoms in three dimensions[6]. The surfaces may be continuous, discontinuous, or even fractal. Depending on the surfaces, the surfaces may produce a structure equivalent to decorating all tiles (or quasi-unit cells) identically or to decorating tiles differently depending on their local environment. Although the descriptions are mathematically related, the quasi-unit-cell picture is simpler in practice: it is much easier to solve for the structure by considering atomic rearrangements within a single quasi-unit cell in real, three-dimensional space than by considering simultaneously decorations or two or more tiles or by imagining surfaces in five or six dimensions.

To test the quasi-unit-cell hypothesis, we consider $Al_{72}Ni_{20}Co_8$, one of the best-characterized quasicrystal materials. $Al_{72}No_{20}Co_8$ is an example of a decagonal phase; that is, a structure consisting of a periodic stack of ten-fold symmetric quasiperiodically ordered layers. Viewed along the periodic axis, the solid has the same symmetry as a Penrose tiling or an overlapping decagon structure. Hence it can be modelled as a columnar stacking of prisms with the shapes of Penrose tiles or decagons. Although quasicrystalline Al–Ni–Co has been studied for nearly a decade, deciphering its structure has been challenging for materials science reasons. The quasicrystal phase was originally found in a wide compositional range[7]. High-resolution transmission electron microscopy revealed decagonal cluster columns roughly 2 nm across[8]. Models of the structure based on two Penrose rhombus tiles, the Penrose six-tile pentagonal set[9,10] and random packing of decagons were proposed on the basis of this early data[11]. In random packing, there are no rules which force the decagons into a unique structure, so infinitely many distinct configurations are possible. (Similar random cluster packing models have been developed for other quasicrystalline materials with decagonal and icosahedral symmetry[12–14].) Although the random cluster packing models and the quasi-unit-cell picture discussed here share the idea of building the atomic structure from a repeating unit, they differ in three important ways: first, the random decagon clusters do not cover the entire structure; second, the random decagon clusters are imperfectly ordered and their arrangement is not unique; and third (in most cases), the random decagon clusters contain an atomic configuration that is five- or ten-fold symmetric.

But it has recently become apparent that, over most of the compositional and temperature range, one obtains an inhomogeneous mixture of structures[15–17]. The ideal, high-perfection phase